

## Modification of Hydroxyapatite/gelatin Nanocomposite with the Addition of Chondroitin Sulfate

Myung Chul Chang<sup>\*,\*\*†</sup>

<sup>\*</sup>Department of Materials Science & Engineering, Kunsan National University, Kunsan 573-701, Korea

<sup>\*\*</sup>Department of Restorative Science [MDRCBB], School of Dentistry, University of Minnesota, Minneapolis, MN 55126, USA

(Received September 23, 2008; Revised October 14, 2008; Accepted October 16, 2008)

### ABSTRACT

In the preparation of hydroxyapatite (HAp)/gelatin (GEL) nanocomposite, GEL matrix was modified by the introduction of chondroitin sulfate (ChS) to obtain a strongly organized composite body. The formation reaction of the HAp/GEL-ChS nanocomposite was then investigated via XRD, DT/TGA, FT-IR, TEM and SEM. The organic-inorganic interaction between HAp nanocrystallites and GEL molecules was confirmed from DT/TGA and FT-IR. According to the DT/TGA results, the exothermal temperature zone between 300 and 550°C showed an additional peak temperature that indicated the decomposition of the combined organics of the GEL and ChS. From the FT-IR analysis, calcium phosphate (Ca-P) was covalently bound with the GEL macromolecules modified by ChS. From TEM and ED, the matrix of the GEL-ChS molecules was mineralized by HAp nanocrystallites and the dense dried nanocomposite body was confirmed from SEM micrographs.

**Key words :** Hydroxyapatite-gelatin nanocomposite, Chondroitin sulfate, Modification, Organic-inorganic interaction

### 1. Introduction

Hydroxyapatite (HAp:  $\text{Ca}_{10}(\text{PO}_4)_6(\text{OH})_2$ ) has been intensively investigated as a bone substitute due to its similar biocompatibility and osteoconductivity to bone.<sup>1-3)</sup> Calcified tissue, such as bone and teeth, is basically considered a biologically and chemically bonded composite between HAp nanocrystals and type-I collagen. Bone is an extracellular matrix mainly composed of HAp nanocrystals and COL fibers in which the HAp nanocrystals align their c-axes with the COL fibers.<sup>4,5)</sup> As an artificial bone substitute, HAp-embedded gelatin (GEL) nanostructure<sup>6,7)</sup> has been reproduced using a biomimetic<sup>8-11)</sup> coprecipitation reaction of HAp nanocrystals in a soluble GEL matrix.<sup>12,13)</sup> Such a composite would be especially advantageous for application as a bone substitute; hydroxyapatite is one of the major constituents of hard tissue. There have been some difficulties to attain sufficient mechanical strength and a proper pore size compared to biological bone. The properties of biological bone tissue<sup>14)</sup> are essentially based on the organic-inorganic interaction between calcium phosphate (Ca-P) and the protein matrix, which consists of each type of COL, glycosamine or other proteins. The large quantities of chondroitin sulfate (ChS) found on aggrecan are thought to play an important role in the hydration of articular cartilage. The resilience of cartilage results from the ChS chains in proteoglycan.<sup>15)</sup> The ChS is part of a large protein mole-

cule (proteoglycan) that gives cartilage its elasticity.

In this report, the GEL matrix was modified with ChS and the organic-inorganic interaction between the GEL-ChS matrix and HAp was investigated in the HAp/GEL-ChS nanocomposite. The prepared slurry paste was very sticky compared to that of the HAp/GEL nanocomposites<sup>6,7)</sup> and a dense dry body was obtained. The organic-inorganic interaction between the Ca-P and the GEL matrix was affected by the addition of ChS molecules. The organic-inorganic interaction between the GEL and ChS greatly contributed to the mineralization of the GEL macromolecule as a result of the HAp phase.

### 2. Materials and Methods

The details of the preparation process of the HAp/GEL nanocomposite are available in the literature.<sup>6,7)</sup> The precursors used here were  $\text{CaCO}_3$  (Alkaline analysis grade, Wako, Japan),  $\text{H}_3\text{PO}_4$  (AP grade, Wako, Japan), GEL (Unflavored, Natural Food Inc., Canada) and chondroitin sulfate (Dermatan, Aldrich). Pure  $\text{Ca}(\text{OH})_2$  was obtained through the hydration of  $\text{CaO}$  calcined at 1150°C for 3 h. The slurry for the HAp/GEL composite was prepared using the simultaneous titration method with peristaltic pumps, a water bath and a pH controller (Bukert 8280H, Germany). The amount of  $\text{Ca}(\text{OH})_2$  and  $\text{H}_3\text{PO}_4$  was calculated to formulate 10 g of HAp. A homogeneous suspension of  $\text{Ca}(\text{OH})_2$  in DI water was prepared after 12 h stirring in a beaker. Three grams of GEL and 100 mg of chondroitin sulfate (ChS) were dissolved in DI water with  $\text{H}_3\text{PO}_4$  at 37°C. A homogeneous suspension of  $\text{Ca}(\text{OH})_2$  of 2 liters and an aqueous solution of

<sup>†</sup>Corresponding author : Myung Chul Chang

E-mail : mcchang@kunsan.ac.kr

Tel : +82-63-469-4735 Fax : +82-63-466-2086

GEL and  $H_3PO_4$  ChS of 1.5 liters were simultaneously added to the reaction vessel through peristaltic pumps. The sample name was coded as HG3-ChS. As controls, HG3 denotes the HAp/GEL nanocomposite sample prepared using 3 g of GEL, and HAP is the HAp sample prepared without GEL. After a coprecipitation reaction, the total volume became 4 liters through a pH adjustment. During the co-precipitation process, the temperature and pH of the reaction solution in the vessel were set and maintained at 37°C and 8.0, respectively. After the reaction, the obtained slurry was aged at 37°C for 24 h. A part of the slurry was used for the TEM observation and the microstructures were characterized by transmission electron microscopy (TEM, JEOL, Japan). The precipitated slurry was then passed through a glass filter. The final cakes were dried naturally at 25°C in air, and a chemical interaction between the HAp crystallites and the functional groups of the GEL-ChS matrix template was estimated using diffuse reflectance FT-IR (Magna 750R, Nicolet, USA) on the crushed powders. The diffusive reflectance of the IR was measured for powder specimens diluted with KBr powder of spectroscopic grade (Spectratech) by one tenth: background noise was corrected with pure KBr data. In order to determine the precise spectral constituents, the band positions were analyzed using GRAMS AI(7.0) (Thermo Galactic, Salem, USA). The microstructure of the dry body was characterized via scanning electron microscopy (SEM, JEOL, Japan). Thermal analysis (TG-DTA TG8120, USA) was carried out on the dried samples. The measurements were done between 25°C and 1200°C at a heating rate of 10°C/min. All experiments were carried out in platinum pans in an air atmosphere.  $Al_2O_3$  powders (10 mg) were used as a reference.

### 3. Results and Discussion

#### 3.1. XRD

In Fig. 1, the crystal development in HG3-ChS was identified as HAp (JCPDS card 9-432), and the XRD pattern was found to be similar to that of HG3. The XRD peaks were diffusive. It was not easy to compare the degree of crystallinity because the (201) and (211) peaks were overlapped with the (002) and (112) peaks, respectively. As controls, HAP is a typical nanocrystalline HAp, and HG3 is a nanocrystalline composite between the HAp and GEL macromolecules.<sup>6,7</sup> The shift of the (002) peak in HG3-ChS may be affected by the organic-inorganic interaction between the complex molecules of GEL-ChS and the nuclei of the HAp crystallites. It was noted that the XRD intensity of HG3-ChS and HG3 was much lower than that of HAP. The reason has been explained as a heterogeneous nucleation of HAp clusters in the GEL matrix template.<sup>6,7,14</sup> That is, number of nucleation sites in the GEL molecules results in a lower likelihood of crystal growth.<sup>6</sup> The precipitated product in HG3-ChS may be a nanocomposite between the HAp nanocrystallites and the GEL-ChS matrix. This can be confirmed from DT-TGA, FT-IR and TEM with electron diffraction (ED).

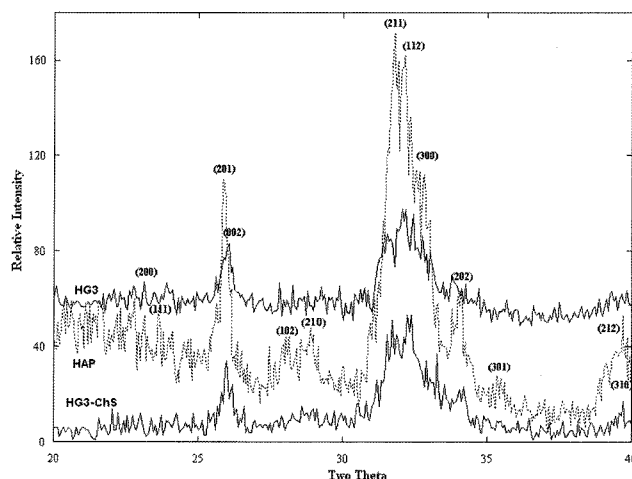


Fig. 1. XRD pattern for HG3-ChS, HG3 and HAP. It shows the mineralization of HAp phase in the combined matrix of GEL with ChS. The crystal development of calcium phosphate of HG3-ChS is very fine, compared to HAP sample.

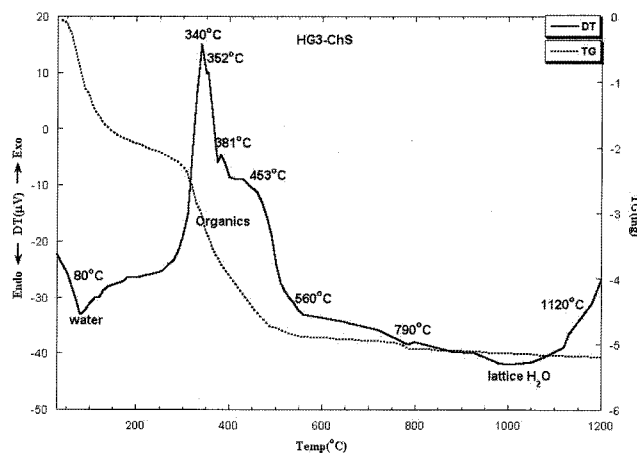
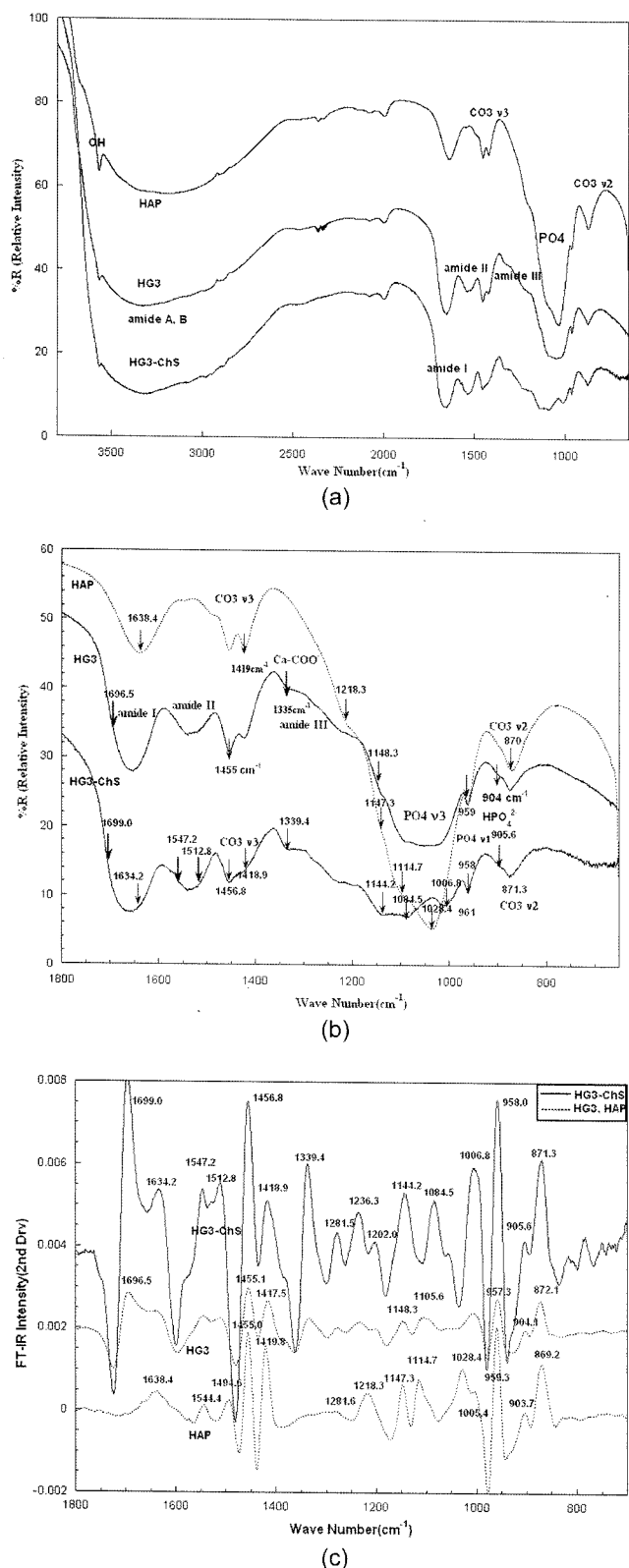


Fig. 2. DT and TG thermal analysis for HG3-ChS. The noted temperature in the Figure indicates the phase change and/or decomposition. From DT and TG it shows the decomposition of organics between 300°C and 500°C.

#### 3.2. DT-TGA

From the DT-TGA for HG3-ChS in Fig. 2, an endothermic peak appears at approximately 80°C, indicating the existence of absorbed water. The DT/TGA curves show similar thermal analysis spectra for the HAp/GEL nanocomposite.<sup>6</sup> There are exothermic peaks between 300 and 550°C. The organic components of HG3-ChS are dissociated with an increase in the temperature. Carbon dioxide is released from carbonate in the HAp phase above 790°C and the crystal lattice water eventually disappears at approximately 980°C. There are several steps in the decomposition of the organic components in HG3-ChS, including 340, 352, 381 and 453°C. This is caused by the decomposition of the GEL, ChS and/or the combined molecules. In the HAp/GEL nanocomposite, three temperature zones of T1, T2 and T3 typically appear,<sup>6</sup> but HG3-ChS shows an additional tiny peak



**Fig. 3.** FT-IR spectra for HG3-ChS, HG3 and HAP between 3800 and 650  $\text{cm}^{-1}$  (a). (b) High resolution amide and PO4 spectra between 1800 and 650  $\text{cm}^{-1}$ . The detail spectra analysis was performed for amide spectra and PO4 spectra. (c) Second derivative analysis showing the peak band frequencies through GRAMS AI(7). All of band frequencies were derived from (c).

at 352°C. It appears that the 352°C peak may be caused by the decomposition of ChS. It was considered that the GEL macromolecules were modified by a small amount of ChS that was incorporated into the molecular structure and that the mineralizing clusters of Ca-P phase interacted with the interpenetrating network (IPN) structure of the GEL-ChS complex. This will be discussed further via FT-IR analysis and by micrographs of TEM and SEM.

### 3.3. FT-IR

In Fig. 3(a), HG3-ChS shows that the typical FT-IR spectra are similar to those of the HAP/GEL nanocomposites.<sup>6,7</sup> From Fig. 3(b) comparing the spectral features of HG3-ChS, HG3 and HAP, the organic-inorganic interaction between the Ca-P phase and the organics of the GEL with ChS can be investigated. The amide I, II, III bands were clearly developed in the HG3-ChS and HG3. The 1335  $\text{cm}^{-1}$  band in HG3 shows a spectral pattern, indicating the resonance of the Ca-COO- complex, which is caused by the wagging vibration of proline side chain through covalent bond formation with the HAP phase.<sup>6</sup> The GEL represents the same band<sup>6,13</sup> at 1339  $\text{cm}^{-1}$ , and a red shift of this band exists for a series of HAP/GEL nanocomposites. The lower chemical shift for the 1339  $\text{cm}^{-1}$  band in the GEL is caused by the critically small size of the Hap crystals bound with GEL molecules,<sup>6</sup> suggesting lower energy wagging of the proline side chain. The band peak of HG3-ChS shown in Fig. 3(b) is estimated as 1339.4  $\text{cm}^{-1}$  in Fig. 3(c). The HAP/GEL-ChS nanocomposites are likely to have been formed by the interaction between the critically smaller size of the Hap crystallites and the GEL molecules, which were modified by the addition of ChS.

In Fig. 3(b) PO4 v3, the v1 spectra correspond to the bands from the phosphates of the Ca-P phase or HAP. It was noted that the PO4 spectra pattern of HG3-ChS is much smoother than that of HG3. There was relatively strong interaction between Ca-P and the GEL-ChS matrix and/or there are greater amounts of organized components in the final nanocomposite of HAP/GEL-ChS. From CO3 v3, the v2 bands of the HG3-ChS sample was less carbonated, indicating less potential for the carbonation of the HAP phase due to the highly active interaction between HAP and the GEL-ChS matrix during the coprecipitation stage. The organic-inorganic interaction was likely to be very active to formulate the nanocomposite of HAP/GEL-ChS. This was likely enhanced by the modified molecular architecture of the GEL-ChS. The IPN structure of the GEL-ChS was chemically very efficient to the point that it could coordinate with the  $\text{Ca}^{2+}$  and phosphates in order to form HAP.

Fig. 3(b) shows the critically different bands among HAP, HG3 and HG3-ChS in the range of 1750 and 1450  $\text{cm}^{-1}$ . The amide I, II bands for HG3 and HG3-ChS show the typical organic spectra patterns of HAP/GEL nanocomposites.<sup>6,7</sup> From Fig. 3(c) the spectral peak bands of HG3-ChS appear more clearly compared to those of HG3. The amide II band spectra of HG3-ChS, represented at 1547 and 1512  $\text{cm}^{-1}$ ,

show a more complicated and delicate spectral feature, indicating the possibility of GEL-ChS interaction. The organic-organic interaction<sup>15,16)</sup> between the GEL and ChS sensitively occurred for the HG3-ChS sample. This can also be demonstrated from the PO4 band spectra shown in Fig. 3(b)(c). The smooth spectra for the PO4 v3 band in HG3-ChS indicate a greater amount of organic-inorganic interaction between HAp and the GEL-ChS compared to HG3. Even when 100 mg of ChS were added to 3 g of the GEL matrix, the organic-organic interaction between the GEL and ChS was fairly strong. The clusters of Ca-P were associated with the matrix template of the GEL-ChS mixture; therefore, the organic-inorganic interaction was strongly induced. The smoothness of the spectral feature of HG3-ChS was close to that of the HG5 sample,<sup>6)</sup> which was prepared using 5 g of GEL. The incorporation of ChS into the GEL matrix contributed to the increase of the organic-inorganic interaction between HAp and the organic matrix of the GEL-ChS mixture. A small amount of ChS considerably enhanced the organic-organic interaction between GEL and ChS, indicating the formation of the IPN structure. The consistency of the obtained slurries paste was very sticky; the high degree of toughness of the dry body resulted from the enhanced organic-inorganic interaction.

Before the coprecipitation process, the GEL powders were mixed with ChS powders in an aqueous solution of  $H_3PO_4$  at 37°C. As the GEL and ChS dissolved in phosphoric acid water, the molecules of GEL and ChS became phosphorylated; therefore, a molecular mixture formed among the phosphorylated molecules.<sup>17)</sup> The mixture of the phosphorylated molecules will become the matrix template for the mineralization by the HAp clusters. From the DTA spectrum in Fig. 2, showing the decomposition of the organics, there is an additional tiny peak beside the three typical peak temperatures of T1, T2, and T3. During the coprecipitation of HAp in the GEL-ChS matrix, ionic clusters of Ca-P are coordinated with the chemically combined GEL-ChS molecules to form the HAp/GEL-ChS nanocomposites. This can be confirmed from the TEM morphology with ED.

From HG3-ChS in Fig. 3(b), there is a small  $HPO_4^{2-}$  band,

indicating a small amount of reaction product between  $HPO_4^{2-}$  and the GEL-ChS matrix. From Fig. 3(c), the  $HPO_4^{2-}$  band of HG3-ChS is centered at  $905.6\text{ cm}^{-1}$ , which was shifted from the band of HAp at  $903.7\text{ cm}^{-1}$ . HAp shows the strong spectral intensity of the  $HPO_4^{2-}$  band relative to those of HG3 and HG3-ChS. As the  $H_3PO_4$  dissolved in DD water, triprotic phosphates kinetically formed, including monobasic ( $H_2PO_4^-$ ), dibasic ( $HPO_4^{2-}$ ) and/or tribasic ( $PO_4^{3-}$ ) phosphate ions.<sup>17)</sup> These basic ions are coordinated with side chains of the amide in the GEL macromolecules. Normally,  $HPO_4^{2-}$  at  $903\text{ cm}^{-1}$  indicates the existence of the OCP phase during the mineralization stage.<sup>14,18)</sup> The HAp/GEL nanocomposite samples showed the  $HPO_4^{2-}$  band spectra,<sup>6)</sup> and the OCP phase<sup>19)</sup> was regularly observed under TEM. However, the OCP phase for HG3-ChS via TEM observations was not observed. In ChS, with its carboxyl group in the sulfate chain, interaction can occur to form the Ca-COO bond. This can be confirmed from the  $1339.4\text{ cm}^{-1}$  band, indicating the Ca-COO bond. The  $1339.4\text{ cm}^{-1}$  spectra band of HG3-ChS is fairly strong compared to HG3. The molecular structure of the GEL was modified via organic coordination using ChS, and/or the single ionic  $Ca^{2+}$  from  $Ca(OH)_2$  in DD water may be quickly consumed through the interaction with the -COO sites of the GEL molecules and ChS molecules. The HAp phase will be formed mostly through the reaction with  $PO_4^{3-}$ , and there is kinetically not enough time for the diffusion of  $HPO_4^{2-}$  for the reaction to formulate OCP. This is another example of evidence for the organic-organic interaction between the GEL and ChS molecules in phosphoric water.

### 3.4. TEM

Fig. 4 shows TEM micrographs of the slurries of the HG3-ChS sample. In Fig. 4(b), which is a magnified view of Fig. 4(a), needle-shaped crystallites can be observed. The crystallites in Fig. 4(b) are the typical HAp phase from ED, which appear as clear ring spots. The ring patterns appear on the plane of (002), (210) and (112), corresponding to the HAp phase. The needle crystallites clearly show the nanocomposites of the HAp phase in the mixture matrix of the

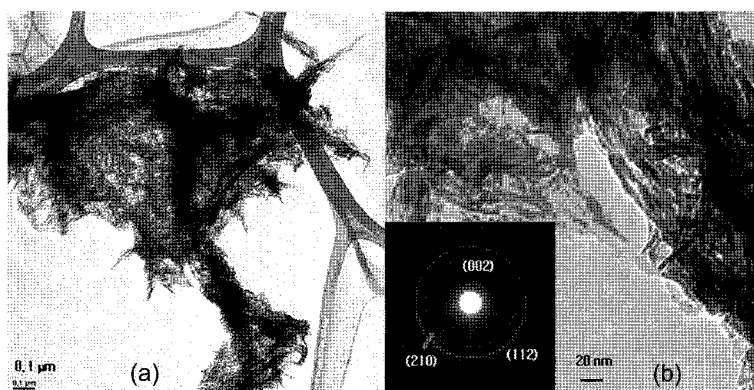


**Fig. 4.** TEM micrographs for HG3-ChS. (a) stuffs of needle-shaped particle composites of HAp/GEL-ChS (b) fine image of needle particle composites with ED, indicating the HAp phase. The clear spots of HAp crystallites are shown in the ring pattern. Each needle particle is the nanocomposite of HAp/GEL-ChS.

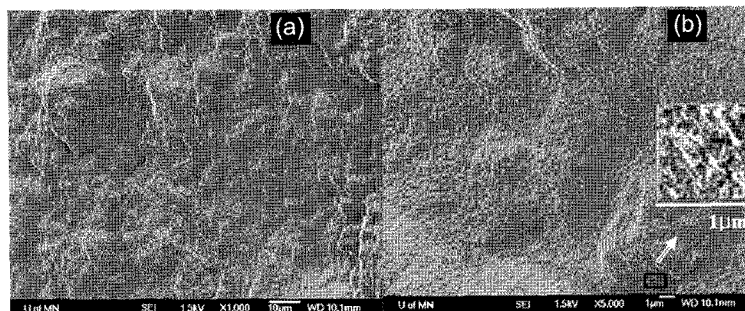


**Fig. 5.** SEM micrographs for HG3-ChS. (a) low magnification picture. (b) high magnification picture, showing the very fine and dense microstructure as a reason of higher toughness. A magnified picture of the arrowed rectangle region shows a dense microstructure in the right side of (b). The scales bars are 10  $\mu\text{m}$  and 1  $\mu\text{m}$  for (a) and (b), respectively.

GEL-ChS, as confirmed from DT and FT-IR. The organic-organic interaction in the final GEL-ChS matrix could be confirmed via FT-IR analysis, as shown in Fig. 3.

### 3.5. SEM

From the SEM micrographs in Fig. 5, the dense composite body can be observed. In the magnified image in Fig. 5(a) shown again in Fig. 5(b), the dense microstructure can be confirmed. The inset in Fig. 5(b) is a magnified image of the rectangular region indicated by the arrow. The higher toughness body of the HG3-ChS samples resulted from the formation of the very sticky slurry during the coprecipitation stage.

In conclusion, two key points can be summarized in this report. The organic-inorganic interaction between the HAP and GEL-ChS matrix was analyzed using FT-IR and DT/TG. The organic-organic interaction between the GEL macromolecules and ChS molecules was analyzed using FT-IR analysis with GRAMS AI (7.0). In order to develop the micrometer-sized pore in the dense tough body, it is necessary to control both factors of the organic-inorganic interaction and the organic-organic interaction. The organic-inorganic interaction is suitable for the control of the toughness and density of the nanocomposite. The organic-organic interaction will also be suitable for the control of matrix organic templates and for the formation of micrometer-sized pores. A polymer precursor can be used for the modification of the GEL, as was reported using PVA and PAA.<sup>20,21</sup> In order to obtain better toughness and micrometer pores, it is necessary to elucidate the organic-organic interaction mechanism between the GEL and another organic material such as a protein, proteoglycan, or polymer.

## 4. Conclusion

A dense dry product of the HAP/GEL-ChS nanocomposite was obtained. The SEM microstructure showed the dense composite crystallites of HAP in the GEL-ChS matrix. The feasible toughness was found to have resulted from the organic-inorganic interaction between the HAP and the organic matrix of the GEL and ChS. Organic-organic interaction between GEL macromolecules and ChS was also con-

firmed.

## REFERENCES

1. W. B. Brown, J. P. Smith, J. R. Rehr, and A. W. Frazier, "Octacalcium Phosphate and Hydroxyapatite," *Nature*, **196** [4859] 1048-55 (1962).
2. R. A. Young, "Biological Apatite vs. Hydroxyapatite at the Atomic Level," *Clinical Orthopedics*, **113** 249-60 (1975).
3. A. Ascenzi and G. H. Bell, in "Bone as a Mechanical Engineering Problem, The Biochemistry and Physiology of Bone; Bone GH, editor," vol. 1, pp. 311-52, Academic Press, New York, 1972.
4. B. B. Doyle, E. G. Bendit, and E. R. Blout, "Infrared Spectroscopy of Collagen and Collagen-like Peptides," *Biopolymers*, **14** 937-57 (1975).
5. C. F. Nawrot and D. J. Campbell, "A Chromatograph Study of the Relative Affinities of Rat Bone and Skin Collagen  $\alpha$  1 chains for hydroxyapatite," *J. Dent. Res.*, **56** [8] 1017-22 (1977).
6. M. C. Chang, C-C Ko, and W. H. Douglas, "Preparation of Hydroxyapatite-gelatin Nanocomposite," *Biomaterials*, **24** 2853-62 (2002).
7. M. C. Chang, Douglas W. H., and Tanaka J, "Organic-inorganic Interaction and the Growth Mechanism of Hydroxyapatite Crystals in Gelatin Matrices between 37 and 80°C," *J. Mater. Sci. Mater. Med.*, **17** 387-96 (2006).
8. S. Mann and G. A. Ozin, "Synthesis of Inorganic Materials with Complex Form," *Nature*, **365** 499-505 (1976).
9. S. Mann, D. D. Archibald, J. M. Didymus, T. Douglas, B. R. Heywood, F. C. Meldrum, and J. R. Nicholas, "Crystallization at Inorganic-organic Interfaces: Biomaterials and Biomimetic Synthesis," *Nature*, **382** 313-18 (1993).
10. A. L. Boskey, "Will Biomimetics Provide New Answers for Old Problems of Calcified Tissues?," *Calcif. Tissue Int.*, **63** 179-82 (1998).
11. S. I. Stupp and P. V. Braun, "Molecular Manipulation of Microstructures: Biomaterials, Ceramics, and Semiconductors," *Science*, **277** 1242-48 (1997).
12. A. G. Word and A. Courts, "The Science and Technology of Gelatin," *Academic Press*, London, 1977.
13. A. Veis, "The Macromolecular Chemistry of Gelatin," *Academic Press*, London, 1964.
14. R. Z. LeGeros, "Calcium Phosphates in Oral Biology and

- Medicine. In: Monographs in Oral Science," vol. 15, pp. 1-129, Kager AG, Basel, Switzerland, 1998.
15. M. L. Chavez, "Glucosamine Sulfate and Chondroitin Sulfates," *Hosp. Pharm.*, **32** [9] 1275-85 (1997).
  16. J. Clarke and A. R. Fersht, "Engineered Disulfide Bonds as Probes of the Folding Pathway of Barnase: Increasing the Stability of Proteins against the Rate of Denaturation," *Biochemistry*, **32** [16] 4322-29 (1993).
  17. D. Corbridge, "Phosphorus: An Outline of its Chemistry, Biochemistry, and Technology. 5th Edition," *Elsevier: Amsterdam*, 1995.
  18. M. S. Tung and D. Skrtic, in "Monogr. Oral. Sci. Vol. 15, Octacalcium Phosphate; Interfacial Calcium Phosphates in Oral Biology and Medicine," p. 112, Kager, Basel, 2001.
  19. M. C. Chang, C-C Ko, and W. H. Douglas, "Conformational Change of Hydroxyapatite/gelatin Nanocomposite by Glutaraldehyde," *Biomaterials*, **24** 3087-94 (2002).
  20. M. C. Chang, C-C Ko, and W. H. Douglas, "Modification of Hydroxyapatite/gelatin Composite by Polyvinylalcohol," *J. Mater. Sci.*, **40** 2753-57 2005.
  21. M. C. Chang, U. K. Kim, and W. H. Douglas, "Modification of Hydroxyapatite/gelatin Nanocomposite using Polyacrylamide," *J. Biomater. Sci. Polymer Edn*, 2008 (to be published).